NASA/TM—2008–215253

An Alternative Method of Specifying Shock Test Criteria

R.C. Ferebee
Marshall Space Flight Center, Marshall Space Flight Center, Alabama

J. Clayton and D. Alldredge
bd Systems, Inc./Subsidiary of SAIC, Huntsville, Alabama

T. Irvine
Vibration Data, LLC., Chandler, Arizona

April 2008

The NASA STI Program…in Profile

Since its founding, NASA has been dedicated to the advancement of aeronautics and space science. The NASA Scientific and Technical Information (STI) Program Office plays a key part in helping NASA maintain this important role.

The NASA STI program operates under the auspices of the Agency Chief Information Officer. It collects, organizes, provides for archiving, and disseminates NASA's STI. The NASA STI program provides access to the NASA Aeronautics and Space Database and its public interface, the NASA Technical Report Server, thus providing one of the largest collections of aeronautical and space science STI in the world. Results are published in both non-NASA channels and by NASA in the NASA STI Report Series, which includes the following report types:

- TECHNICAL PUBLICATION. Reports of completed research or a major significant phase of research that present the results of NASA programs and include extensive data or theoretical analysis. Includes compilations of significant scientific and technical data and information deemed to be of continuing reference value. NASA's counterpart of peer-reviewed formal professional papers but has less stringent limitations on manuscript length and extent of graphic presentations.

- TECHNICAL MEMORANDUM. Scientific and technical findings that are preliminary or of specialized interest, e.g., quick release reports, working papers, and bibliographies that contain minimal annotation. Does not contain extensive analysis.

- CONTRACTOR REPORT. Scientific and technical findings by NASA-sponsored contractors and grantees.

- CONFERENCE PUBLICATION. Collected papers from scientific and technical conferences, symposia, seminars, or other meetings sponsored or cosponsored by NASA.

- SPECIAL PUBLICATION. Scientific, technical, or historical information from NASA programs, projects, and missions, often concerned with subjects having substantial public interest.

- TECHNICAL TRANSLATION. English-language translations of foreign scientific and technical material pertinent to NASA's mission.

Specialized services also include creating custom thesauri, building customized databases, and organizing and publishing research results.

For more information about the NASA STI program, see the following:

- Access the NASA STI program home page at <http://www.sti.nasa.gov>

- E-mail your question via the Internet to <help@sti.nasa.gov>

- Fax your question to the NASA STI Help Desk at 301–621–0134

- Phone the NASA STI Help Desk at 301–621–0390

- Write to:
  NASA STI Help Desk
  NASA Center for AeroSpace Information
  7115 Standard Drive
  Hanover, MD 21076–1320

NASA/TM—2008–215253

An Alternative Method of Specifying Shock Test Criteria

R.C. Ferebee
Marshall Space Flight Center, Marshall Space Flight Center, Alabama

J. Clayton and D. Alldredge
bd Systems, Inc./Subsidiary of SAIC, Huntsville, Alabama

T. Irvine
Vibration Data, LLC., Chandler, Arizona

National Aeronautics and
Space Administration

Marshall Space Flight Center • MSFC, Alabama 35812

April 2008

Acknowledgments

The bulk of this material was written by Joe Clayton from bd Systems and Tom Irvine from Vibration Data, LLC. based on conversations with Robin Ferebee about several test failures experienced during shock testing. Joe conceived of the idea of using wavelets to approximate shock time histories, and Tom Irvine wrote the software to implement the idea. Special thanks to David Alldredge from bd Systems and Rajinder Mehta and Lowery Duvall from Marshall Space Flight Center for reviewing and editing the work..

TRADEMARKS

Available from:

NASA Center for AeroSpace Information
7115 Standard Drive
Hanover, MD 21076–1320
301–621–0390

This report is also available in electronic form at
<https://www2.sti.nasa.gov>

TABLE OF CONTENTS

LIST OF FIGURES

LIST OF TABLES

LIST OF ACRONYMS

ET	external tank
IEA	integrated electronics assembly
ME	main engines
MEE	maximum expected environment
MSFC	Marshall Space Flight Center
PL	probability level
PSD	power spectral densities
RMS	root mean square
SRB	solid rocket booster
SRS	shock response spectrum
STS	Space Transportation System
TM	Technical Memorandum

NOMENCLATURE

A_m	acceleration amplitude of wavelet *m*
C	damping factor
D_m	wavelet displacement
f_m	wavelet frequency
G	acceleration
g	peak acceleration
N_m	number of half-sines
n	number of samples
M_0	mass of exemplar mounting structure
M_1	mass of exemplar chassis
M_2	mass of exemplar substructure
K	stiffness factor of exemplar mounting structure
K_1	stiffness factor of exemplar chassis
K_2	stiffness factor of exemplar substructure
Q	damping value
s	sample standard deviation
t	time(s)
t_{dm}	wavelet time delay
V_0	initial velocity
V_m	velocity of wavelet *m*

NOMENCLATURE (Continued)

W_m	acceleration of wavelet m
$\ddot{x}$	total acceleration
$\overline{x}$	mean value

TECHNICAL MEMORANDUM

AN ALTERNATIVE METHOD OF SPECIFYING SHOCK TEST CRITERIA

1. INTRODUCTION

The Space Shuttle is boosted into orbit by two large 3.3-million-lb thrust solid rocket boosters (SRBs) and three Space Shuttle main engines (ME). Each of these propulsion elements is reusable; the SRBs are qualified for 20 missions. During some of the early Space Shuttle flights, it was discovered that water impact shock levels on the SRBs had been underpredicted. Later flights added extensive flight instrumentation to characterize and map the environments on the SRBs. Since the hardware had flown several times before the discovery of the exceedances and survived, it was decided that the components would not be qualification tested to the new environments; however, any changes to the hardware would have to be qualified depending on the significance of the changes. The SRB integrated electronics assembly (IEA) was selected for qualification due to such a hardware change.

The IEA is rather large for an electronics box: about 4 ft long and 200 lb. There are two per SRB—one in the forward skirt and the other on the external tank (ET) attach ring. The water impact shock response spectrum (SRS) was as specified below:

Table 1. Water impact SRS test criteria.

Water Impact SRS Test Criteria
(All axes, one shock per axis per mission, Q=10)
20 Hz @ 50 g's peak
20 – 70 Hz @ +8 dB/oct
70 – 5,000 Hz @ 250 g's peak

Per Marshall Space Flight Center (MSFC) policy, the criteria were supposed to envelope the actual maximum predicted environment with no additional margin. When a mass simulator using an actual housing was tested to these levels, the cast aluminum housing broke at the box-to-fixture interface. There had been similar flight failures on the aft IEA, but they were due to water pressure from cavity collapse rather than deceleration. The flight data were reviewed further, and the test criteria were reduced to 140 *g* peak. A subsequent test on another housing to the new levels also resulted in a similar failure. Other SRB hardware, such as batteries with nylon housings, was also very difficult to qualify by test using the SRS. Clearly, the test criteria were not representing the actual flight conditions.

The SRS has served the shock and vibration community for years, allowing practitioners the ability to qualify sensitive hardware to harsh aerospace and other shock environments. Previously, the community assumed that if the severity of the SRS synthesized by the shaker is equal to the severity of the SRS measured, then the hardware would have equivalent effects. This was assumed even if the single-degree-of-freedom systems selected as reference in the construction of the SRS do not represent the actual hardware to be tested. Often, if the SRS of measured transients at multiple locations or events characterizes the environment, averaging or enveloping is employed to produce a global SRS. As well served as the community has been by these assumptions over the years, the need is great for SRS testing to evolve in a direction toward reproducing as closely as possible the actual complex transient signatures of the measured excitation. The reasons for doing so include the following:

(1) Lack of repeatability/reproducibility of SRS between laboratories and/or shakers brought about by inadequate instrumentation, anti-aliasing filter characteristics, or alternating current (ac)-coupling strategies.[1]

(2) Neglect of the compliance of the mounting structure, often referred to as spectrum dip, frequently leads to overtesting. This is especially true for global SRS—created by enveloping or averaging-assigned to represent an entire mounting zone for a variety of equipment of different weights, geometries and dynamic characterizations.[2]

(3) SRS construction eliminates phasing information. If the structure being tested is not characterized by a dominant mode in the frequency band of interest, differences between the motion created by the shaker to represent the SRS and the actual transient motion measured can neglect significant coupling between modes.

(4) SRS construction is done using linear idealistic single-degree-of-freedom systems. Nonlinearities in the actual hardware resulting from friction or nonlinear springs created by gapping or other sources often preclude even the dominant modes from responding in a manner capable of being predicted by an idealistic single-degree-of-freedom-system.

Other reasons can be listed with different consequences, but the point would be the same: shock testing needs to duplicate as closely as possible the actual excitation signal. Often, the actual excitation signal is measured by accelerometers mounted directly on the mounting structure. However, these signals cannot be used as direct input into a shaker because integration of the signal would far exceed the stroke length of the shaker. Figure 1 illustrates this by showing the needed stroke length of a shaker required to handle the measured input to the IEA as a result of water impact on STS–6. One common method to reconstruct a measured signal employs a series of damped sinusoids. This method in itself does not preclude significant integrated motion from occurring; however, post-processing algorithms have been developed to remove the accumulation of significant displacement in the integration. These algorithms are cumbersome and a bit unnatural. The use of wavelets allows a more comprehensive and easier-to-implement strategy. Most laboratories today utilize wavelets to construct the SRS, which have inherent net zero displacements, as discussed later. However, these algorithms utilize wavelets to produce an equivalent SRS typically specified by an environment definition determined from the SRS of the measured excitation.

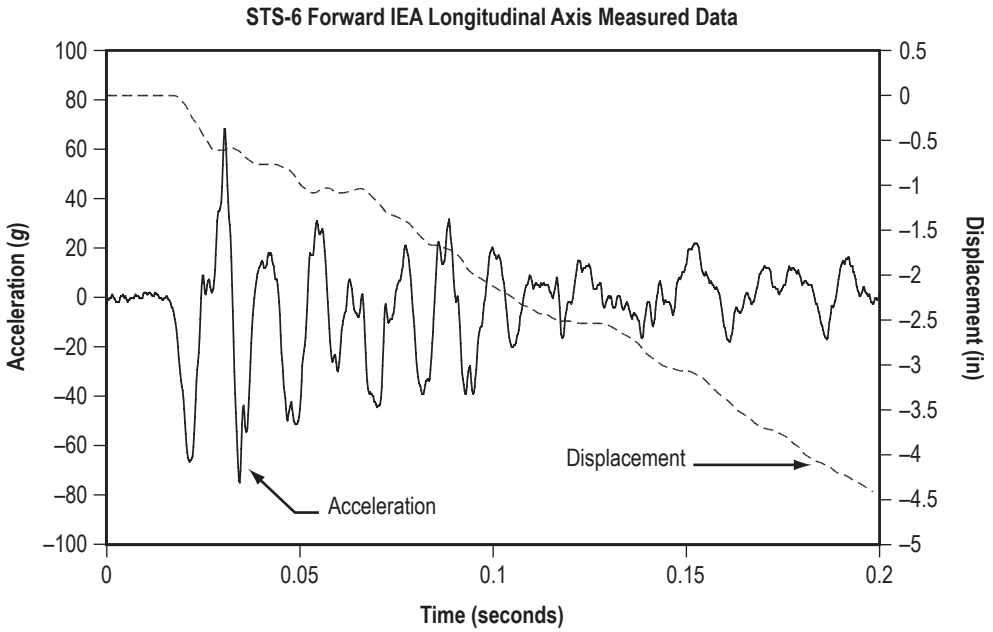

Figure 1. Longitudinal water impact shock data.

It will be the goal of this Technical Memorandum (TM) to prove a need for eliminating where possible the use of the SRS and replace it with a wavelet-generated reconstruction of the measured excitation signal. This TM will also present the reconstruction process and detailed outline of the wavelet algorithm. In cases where the actual excitation is unknown, the SRS is recommended with the caveat that SRS testing is an art, and items (1) through (4) listed above should be considered during its use.

2. OUTLINING THE NEED

The following discussion amplifies the concerns associated with SRS testing pointed out in the introduction. Because analytical examples of data acquisitioning, filtering, etc. do not lend themselves readily to simulations, illustrations of the problems with SRS testing will be limited to spectrum dip, coupling of modes, and structural nonlinearities. The following will also present clarification of how each of these can create problems with traditional SRS testing.

2.1 Spectrum Dip

If the impedance of the mounting structure is large relative to the equipment mounted on it, such as a building mounted to the Earth during an earthquake, the reaction forces to the mounting structure do not have sufficient magnitude to alter the input motion. However, if the equipment mass is large relative to the effective mass of the mounting structure, the inertial forces of the equipment alter the input motion. Consider the two dynamical systems shown in figure 2. The first system is a representation of a chassis (M_1) mounted on some mounting structure (M_0) and a substructure (M_2) mounted inside the chassis. Such a substructure/chassis system could be the multiplexer-demultiplexer mounted inside the IEA. For purposes of clarification, the system depicted in figure 2 will arbitrarily be given the following values:

- M_0 (mass) = 4.33 lbf-s^2/in
- M_1 = 1.51855 lbf-s^2/in
- M_2 = 0.51855 lbf-s^2/in
- K (stiffness) = 1,500,000 lbf/in
- K_1 = 50,000 lbf/in
- K_2 = 25,000 lbf/in
- C (damping) = C_1 = C_2 = 0

If M_0 is given an initial velocity of V_0 = 10 in/s, an SRS of the signal recorded by an accelerometer mounted on M_0 will exhibit peaks to the left and right of the fixed base (infinite impedance) system resonances (fig. 2a). The resonant frequencies of the infinite impedance fixed base system are 22.9 and 44.2 Hz. Figure 3 clearly shows this: fixing mass M_0 results in resonances at 22.9 Hz and 44.2 Hz. Dips can be seen near these two frequencies on the SRS of M_0. Conventional testing will envelop the 18.95 Hz, 34.44 Hz, and 45.78 Hz peaks from an SRS of M_0 and then apply as input to the hard-mounted, two-mass system.

Overtesting is almost a certainty. The infinite impedance model is representative of what will be tested as a result of bolting the test item to a shaker table, but it is an altered model from reality where a compliant mass really exists. Nature reduced the input to the real model at the natural frequencies of the altered model (fixed M_0). However, since testing will be carried out on the altered model, enveloping will add significant energy right where it is most undesirable: at the resonant frequencies of the system being tested (altered model). Overtesting by an order of magnitude would not be uncommon.

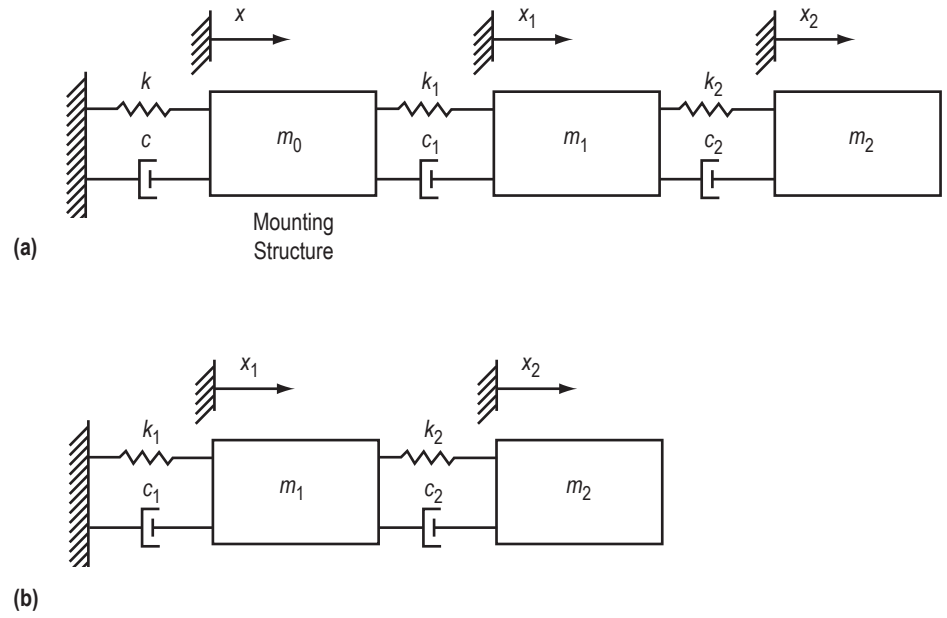

Figure 2. Compliant and infinite impedance models.

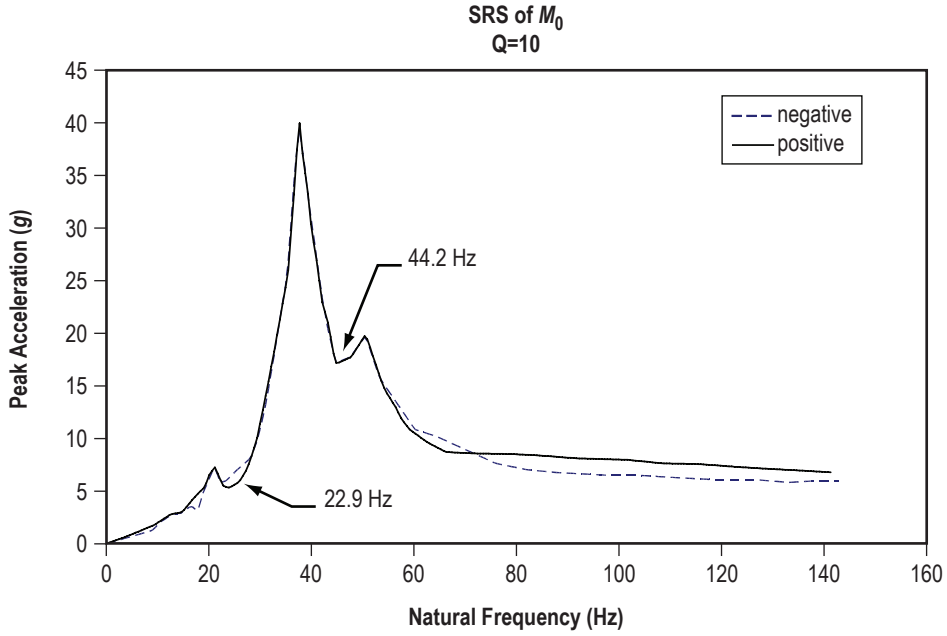

Figure 3. SRS depicting a dip in the spectrum.

Typical shock response spectra represent systems with many degrees of freedom where many dips are enveloped, or better yet, collections of spectra obtained at the same location, each with multiple dips, and enveloped for convenience and necessity. This is also true with vibration environments where the impedance of the mounting structure creates dips in the random vibration power spectral densities (PSD) measured at the base and enveloping creates overtesting concerns with fixed base tests. Force

limited vibration testing has been employed to address this problem.[3] No matter the environment, shock or vibration, these dips are nature's way of naturally reducing the input, and any enveloping results in design SRS and PSDs that are overly conservative. What is needed is a reconstructed signal of the measured base acceleration that inherently possesses the same acceleration waveform, yet yields no appreciable displacement that is capable of being generated by a shaker. Such a shock specification would necessarily include the spectrum dips and preclude over design.

Before leaving this section, it should be mentioned that if the actual motion being specified by the shaker and input into the 'altered model' is close to the exact motion measured at M_0, then the altered is the correct model. This is because specifying the motion at M_0 removes the M_0 degree-of-freedom and fixes the base mass M_0.

2.2 Phasing

The second problem with SRS testing is phasing. Since the definition of SRS removes any phase information by selecting maximums without regard to when they occur in the response, multiple-degree-of-freedom systems with multiple modes will react differently to two different signals that produce similar SRS. The SRS models the responses of individual single-degree-of-freedom systems to a common base input. The natural frequency of each system is an independent variable. The damping value is usually fixed at 5% or equivalently at $Q = 10$. The SRS calculation retains the peak response of each system as a function of natural frequency. No care is taken to account for the time in which the maximum was recorded. The resulting SRS is plotted in terms of peak acceleration (g) versus natural frequency (Hz). Therefore, frequency content is captured, but it should not be considered in any way equivalent to a Fourier solution. For instance, a time history of a pure sine wave pushed through an SRS analyzer would yield significant response values at and near the frequency of the sine wave. A bell shape would result. On the other hand, a Fourier solution would yield a discrete line at the precise frequency of the sine wave. As multiple sine waves were superimposed on one another, the resulting SRS would cause the 'skirts' of these responses to blend into one another and thereby lose precise frequency content information.

A given time history has a unique SRS. On the other hand, a given SRS may be satisfied by a variety of base inputs within prescribed tolerance bands. Figures 4 and 5 depict this. Figure 4 shows three different acceleration time histories, all yielding equivalent SRS. The SRS corresponding to the time histories in figure 4 are shown in figure 5. Therefore, multiple time histories can satisfy a given SRS.

Figure 2 (b) can be used to illustrate the coupling effects the different signals in figure 4 can create as they are input to the base. Using the system as shown in figure 2 and setting the masses and springs to the values outlined in the spectrum dip section results in frequencies of 30 Hz and 80 Hz. If the acceleration time histories, shown in figure 4, are then input, the results are maximum force values that stay within 12%. These force values between the masses are shown in figure 6. However, when the mass and stiffness values are altered to bring the frequencies closer together (26 Hz and 35 Hz) the same signals generate forces that are separated by almost 50%, as shown in figure 7. This result is intuitive in that frequency spacing can either tend to couple results or uncouple them. It should be noted that methods utilizing modal parameters, such as participation factors, are widely used to calculate response values for multiple-degree-of-freedom systems. In such cases, techniques, such as the shock response spectra, attempt to account for the unknown phasing.

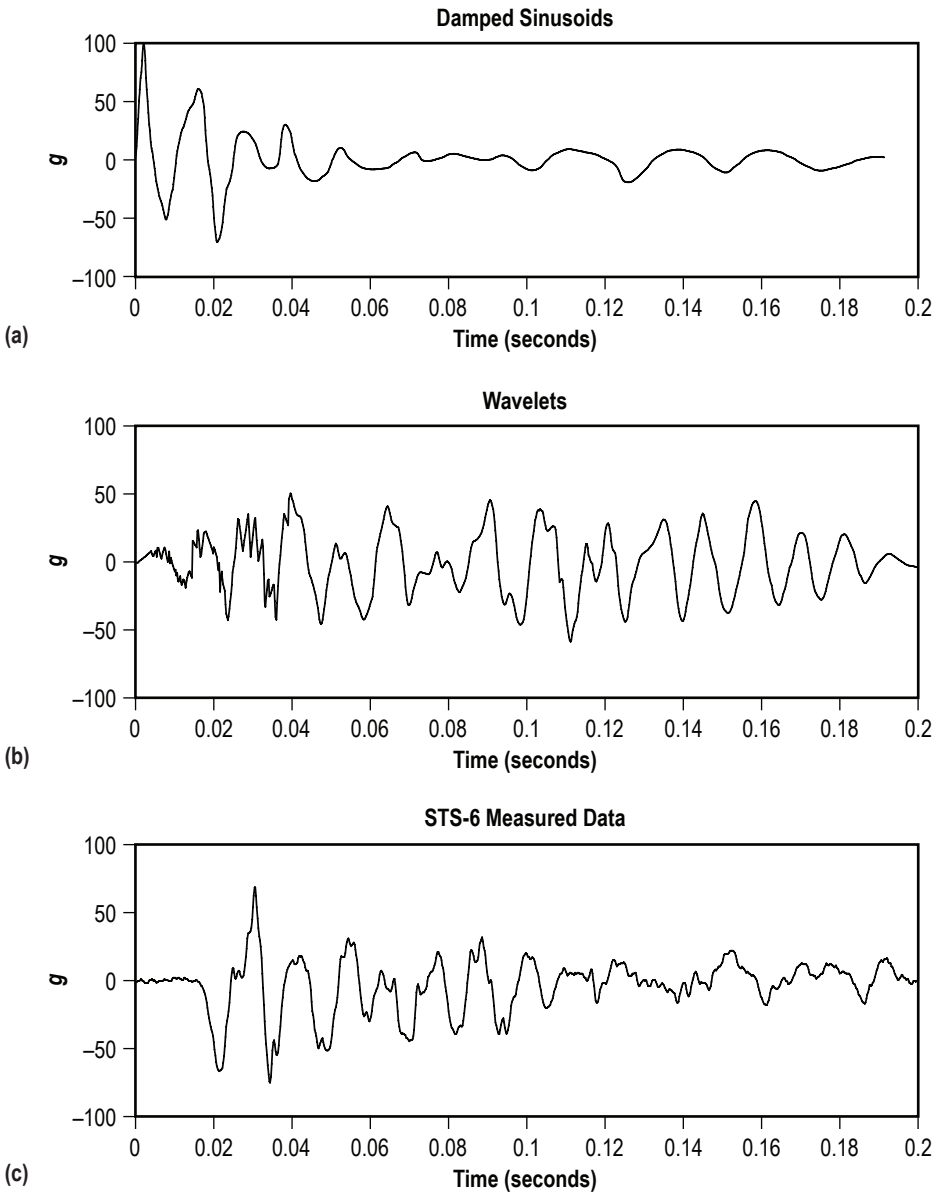

Figure 4. Acceleration histories.

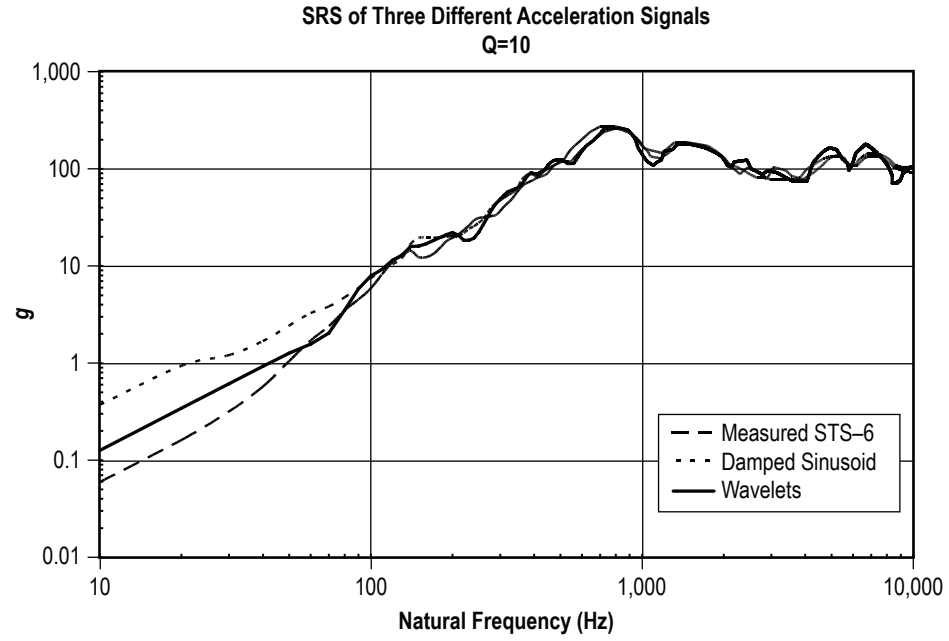

Figure 5. SRS results of three different acceleration signals.

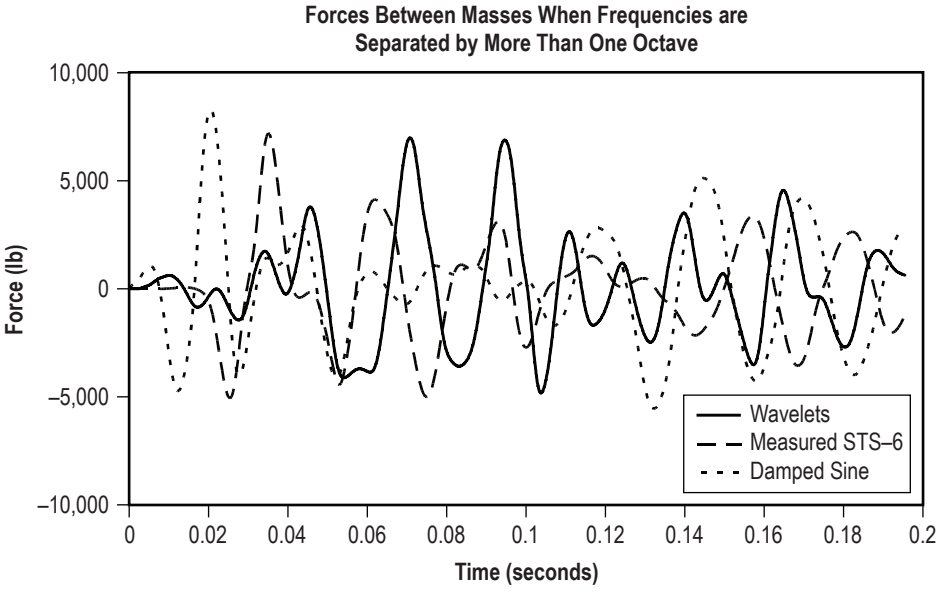

Figure 6. Force levels between M_1 and M_2 ($w_1 = 30$ Hz, $w_2 = 80$ Hz).

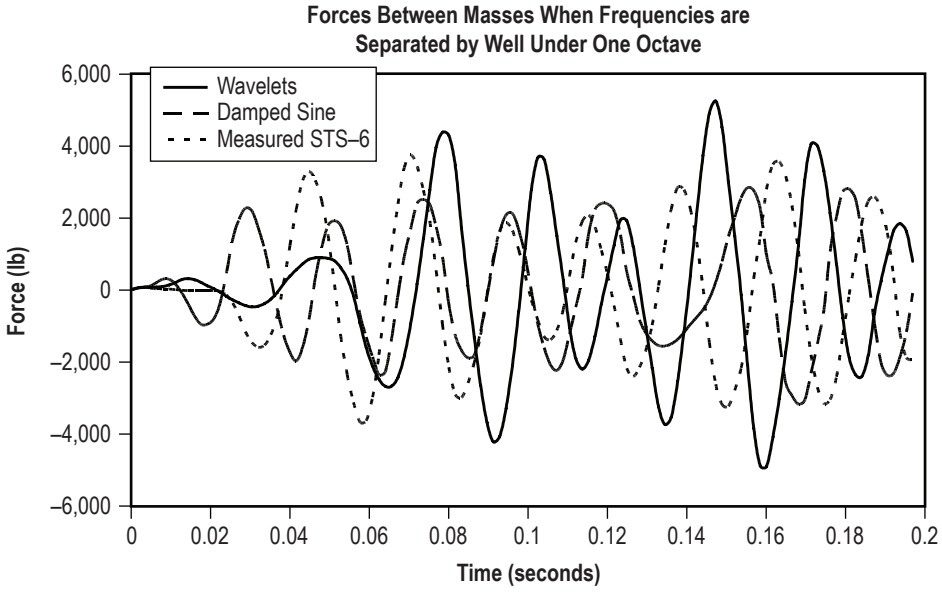

Figure 7. Force levels between M_1 and M_2 ($w_1 = 26$ Hz, $w_2 = 35$ Hz).

2.3 Nonlinearities

It is well understood that all systems in the real world possess some degree of nonlinearity. How much and the source are always the question. It is also understood that analysts, as well as structural test practitioners, circumvent dealing with nonlinear phenomena by making linear assumptions. One such assumption can be found in the very definition of shock spectra where linear single-degree-of-freedom systems are responding to a specified input. Shock spectra treatment can be off by a large amount if the real structure is mounted on nonlinear shock mounts or possesses significant frictional damping.

The above discussions serve to point out that multiple reasons exist to bypass SRS methodologies if possible. The most accurate and realistic alternative is to reconstruct the actual time history waveform. As has already been mentioned, several ways exist to do this, with the most notable involving the use of damped sinusoids and wavelets. Wavelets offer the better and more elegant of the two in that they possess the inherent quality of yielding zero net displacements and velocities. While this conclusion can be reached using postprocessing algorithms with damped sinusoids, it is unnatural. This TM will present a methodology for synthesizing a time history using a wavelet series. The synthesized time history will represent a measured shock time history. The synthesized time history could then be applied as a base input on a shaker table to a test item.

Recall that zero-net displacement and zero-net velocity are necessary characteristics for shaker shock tests. Furthermore, this condition is satisfied by each individual wavelet, as well as by the complete series. This wavelet reconstruction method is an alternative to traditional SRS methods, in terms of test specification and fulfillment. The wavelet approach may also be used as an extension of the SRS method, satisfying criteria both in the time and natural frequency domains.

3. A RECONSTRUCTION ALGORITHM USING WAVELETS

Most shock specifications in the aerospace industry are given in terms of an SRS. In some cases, specifications are also given in terms of classical base inputs. A third format is drop shock onto a hard surface from a prescribed height.

The SRS models the responses of individual single-degree-of-freedom systems to a common base input. The natural frequency of each system is an independent variable. The damping value is usually fixed at 5%, or $Q = 10$. The SRS calculation retains the peak response of each system as a function of natural frequency, and the resulting SRS is plotted in terms of peak acceleration (g) versus natural frequency (Hz). A given time history has a unique SRS, but a given SRS may be satisfied by a variety of base inputs within prescribed tolerance bands.

For example, consider that an avionics component mounted on a vehicle must withstand a complex oscillating pulse that has been measured during a field test. The data might also come from a flight in the case of a missile or aircraft. The avionics component must be tested in a lab to withstand this base input time history. The measured time history, however, may or may not be reproducible in a test lab.

The measured time history can be converted into an SRS specification. The SRS method provides an indirect method for satisfying the specification by allowing for the substitution of a base input time history that is different than the one measured in the field test. The important point is that the test lab time history must have an SRS that matches the SRS of the field data within prescribed tolerance bands.

There is some concern in the aerospace industry, however, regarding the limitations of the SRS method. In particular, a given avionics component most likely responds as a multiple-degree-of-freedom system. Cumulative fatigue and nonlinear responses are additional concerns. Reproducing an actual measured time history in the lab, when possible, can largely solve these problems. This reconstruction approach is discussed briefly in reference 1 and an excerpt is given in appendix A.[1] Again, this reconstruction can be achieved via wavelets.[4]

3.1 Wavelet Method

For simplicity, assume that the measured time history is within the shaker's limits in terms of frequency and acceleration. Furthermore, assume that the control computer can accept a time history input in ASCII text format. Ideally, the exact measured time history could then be input directly into the control computer. A measured time history, however, almost always has a non-zero net displacement that likely exceeds the shaker's limit. The resulting displacement may be real, but is usually spurious. The wavelet method overcomes this obstacle. Furthermore, the wavelet method yields a mathematically closed-form approximation of the measured signal.

The equation for an individual wavelet is

$$W_m(t) = \begin{cases} 0, \quad \text{for } t < t_{dm} \\ A_m \sin\left[\dfrac{2\pi f_m}{N_m}\left(t - t_{dm}\right)\right]\sin\left[2\pi f_m\left(t - t_{dm}\right)\right], \ \text{for } t_{dm} \le t \le \left[t_{dm} + \dfrac{N_m}{2f_m}\right] \\ 0, \quad \text{for } t > \left[t_{dm} + \dfrac{N_m}{2f_m}\right] \end{cases} \tag{1}$$

where

$W_m(t)$ = acceleration of wavelet m at time t

A_m = wavelet acceleration amplitude

f_m = wavelet frequency

N_m = number of half-sines

t_{dm} = wavelet time delay

Note that N_m must be an odd integer ≥3. The wavelet formula is well established in the vibration test industry, as shown in reference 2. The corresponding velocity and displacement are derived in appendices B and C, respectively. These appendices also give proof that each metric has a net value of zero. The initial velocity and initial displacement are each zero for each wavelet.

The total acceleration ($\ddot{x}$) at time t for a set of n wavelets is

$$\ddot{x}(t) = \sum_{m=1}^{n} W_m(t) \ . \tag{2}$$

The coefficients required to match a given time history can be determined via brute force trial-and-error using random number generation. The approach is to select the wavelet that yields the lowest error when subtracted from the measured data. Over 100,000 iterations may be used for each wavelet. The optimized wavelet is then subtracted from the measured signal for the next run. This process is then repeated for each additional wavelet.

3.2 Reconstructing a Single Time History

A sample time history from a Space Shuttle SRB ocean impact is shown in figure 8. An avionics component mounted on the booster must withstand the water impact event because it must be reused in future flights. A series of 60 wavelets was synthesized to model the measured time history. The resulting parameters are shown in appendix D. A further explanation of wavelets is also given in this appendix.

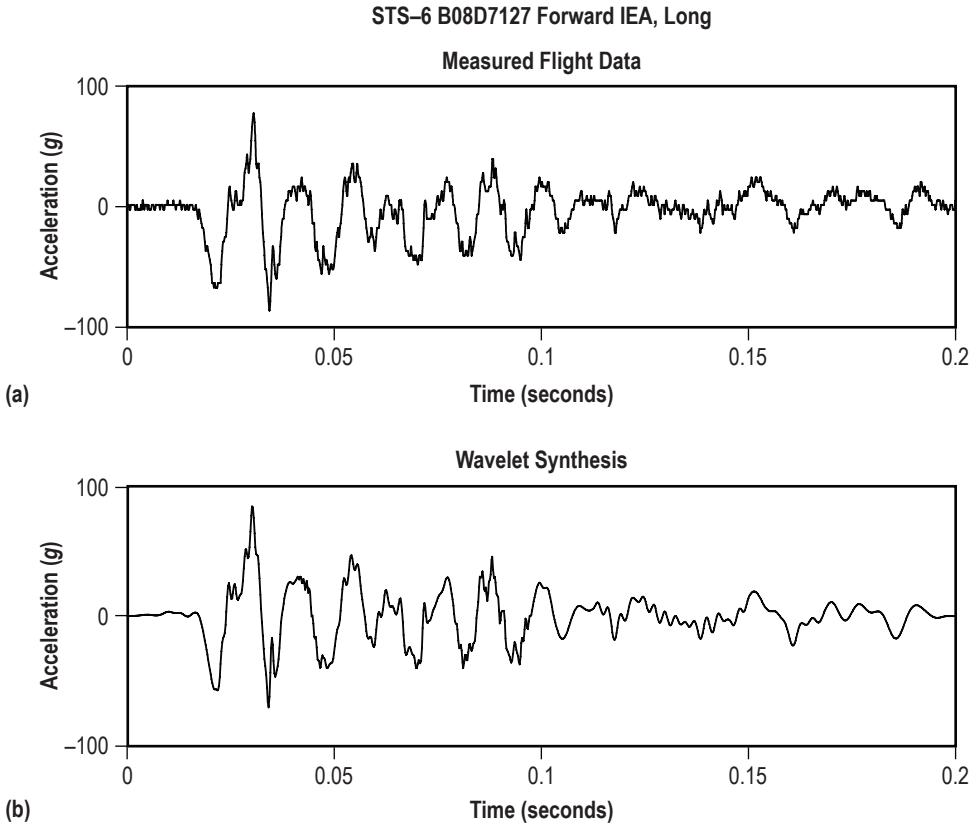

Figure 8. Synthesized time history.

The synthesized time history is also shown in figure 8, and the agreement is close. The measured time history, however, has some high frequency noise that was not modeled.

The synthesized time history in figure 8 could be used as a basis for deriving a maximum expected environment (MEE). An appropriate statistical uncertainty margin should be added as a step in this process. The synthesized waveform is shown in figure 9 along with three of its components. The individual wavelet frequencies could be useful for identifying modal frequencies, complementing other tools, such as the Fourier transform. As demonstrated by figure 10, the shock response spectra comparison is likewise very good.

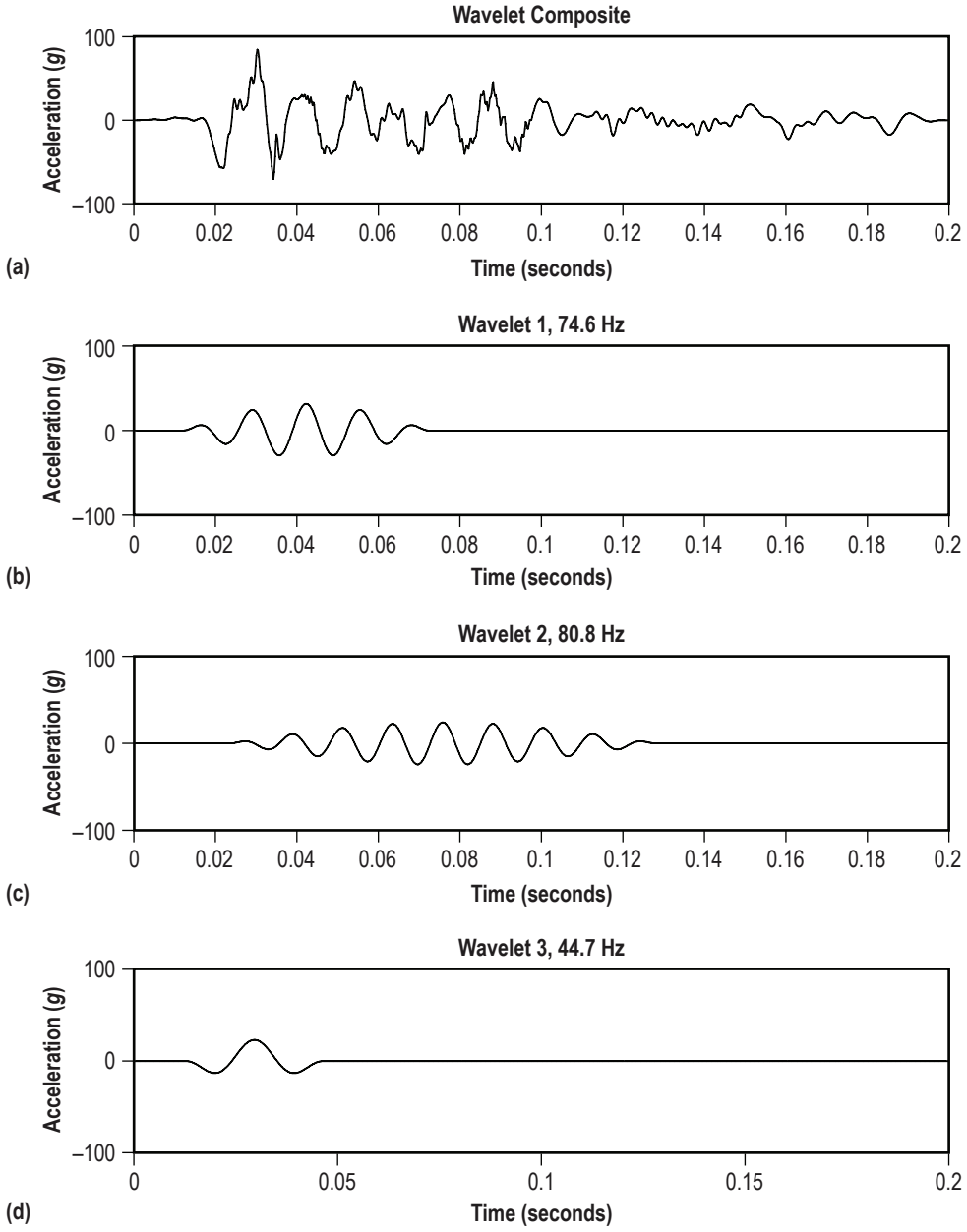

Figure 9. Synthesized waveform with three components.

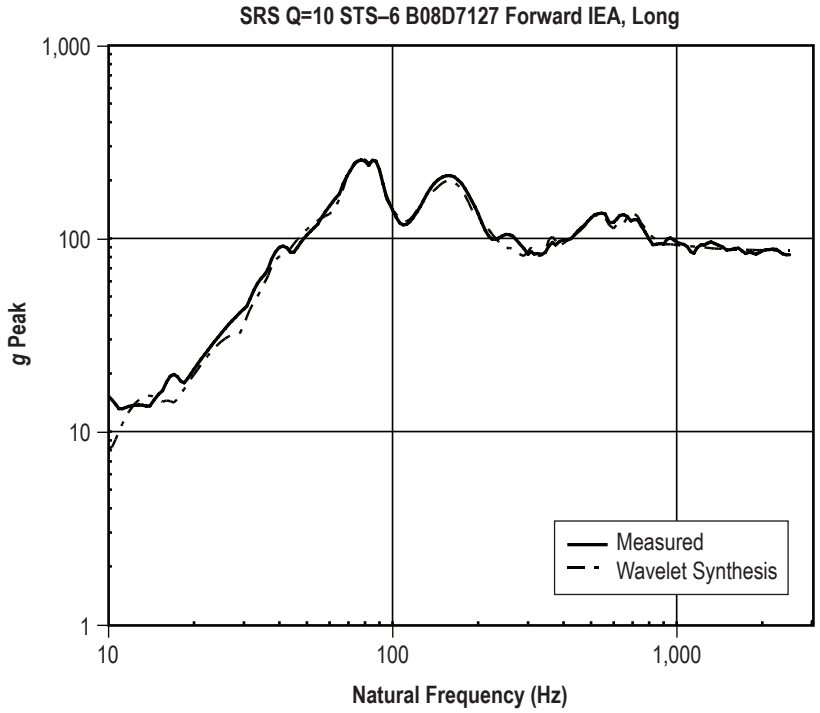

Figure 10. Shock response comparison.

The velocity time history integrated from the acceleration time history is shown in figure 11. The net velocity is zero.

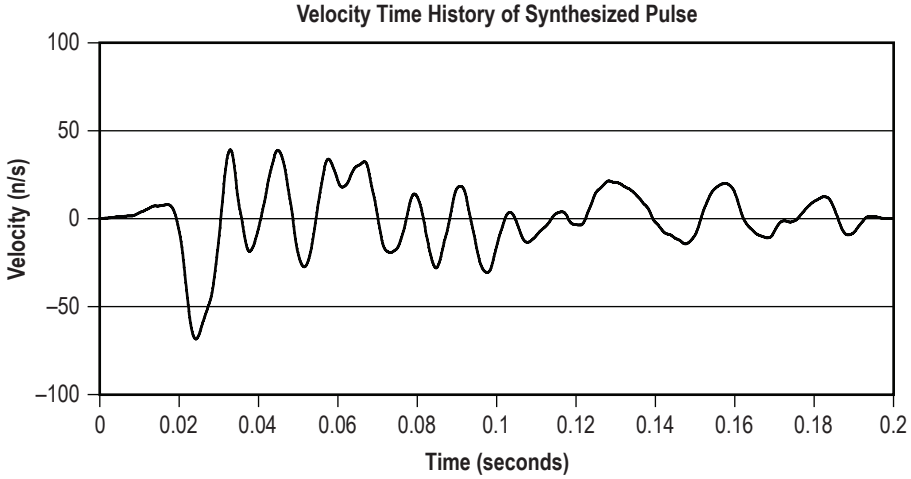

Figure 11. Velocity time history.

The displacement time history double-integrated from the acceleration time history is shown in figure 12. The net displacement is zero.

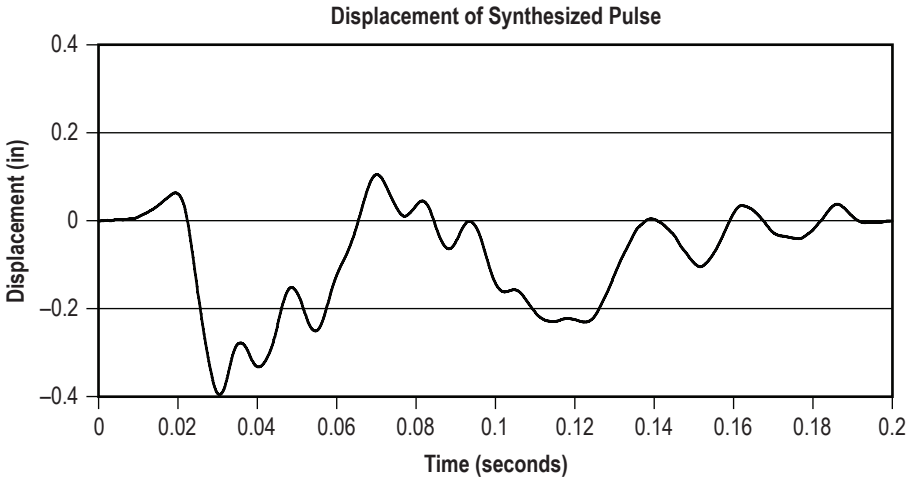

Figure 12. Displacement time history.

3.3 Constructing a Single Time History Representing Multiple Time Histories

Reconstructing a single time history via wavelets is relatively straightforward. Consider a complex case where up to three accelerometers were mounted adjacent to a large avionics component on the rocket booster. Again, the purpose was to record the shock for the water impact event. The accelerometers were mounted in different locations, but each in the longitudinal axis. The goal was to account for spatial variation. Furthermore, data were measured on each of two flights to account for flight-to-flight variation. This is important since the wind conditions, sea state, and other parameters may vary significantly from one flight to the next.

The four measured time histories are shown in figure 13. Note that signal 2 is the same as that shown in figure 1. The raw data corresponding to the fourth signal appeared to be clipped. A cubic spline method was used to estimate the true signal.

The four shock response spectra are shown in figure 14. A P95/50 envelope is also shown. The P95/50 method is taken from references 3 and 4 and a brief summary is given in appendix E. The P95/50 method is one of several possible enveloping techniques for establishing an MEE level. The wavelet reconstruction method may be used with other envelope types.

The next step is to derive a time history pulse that satisfies two goals: the SRS of the synthesized pulse must match the P95/50 SRS within ±3dB tolerance bands, and the synthesized pulse must resemble the composite of the measured time histories in figure 15.

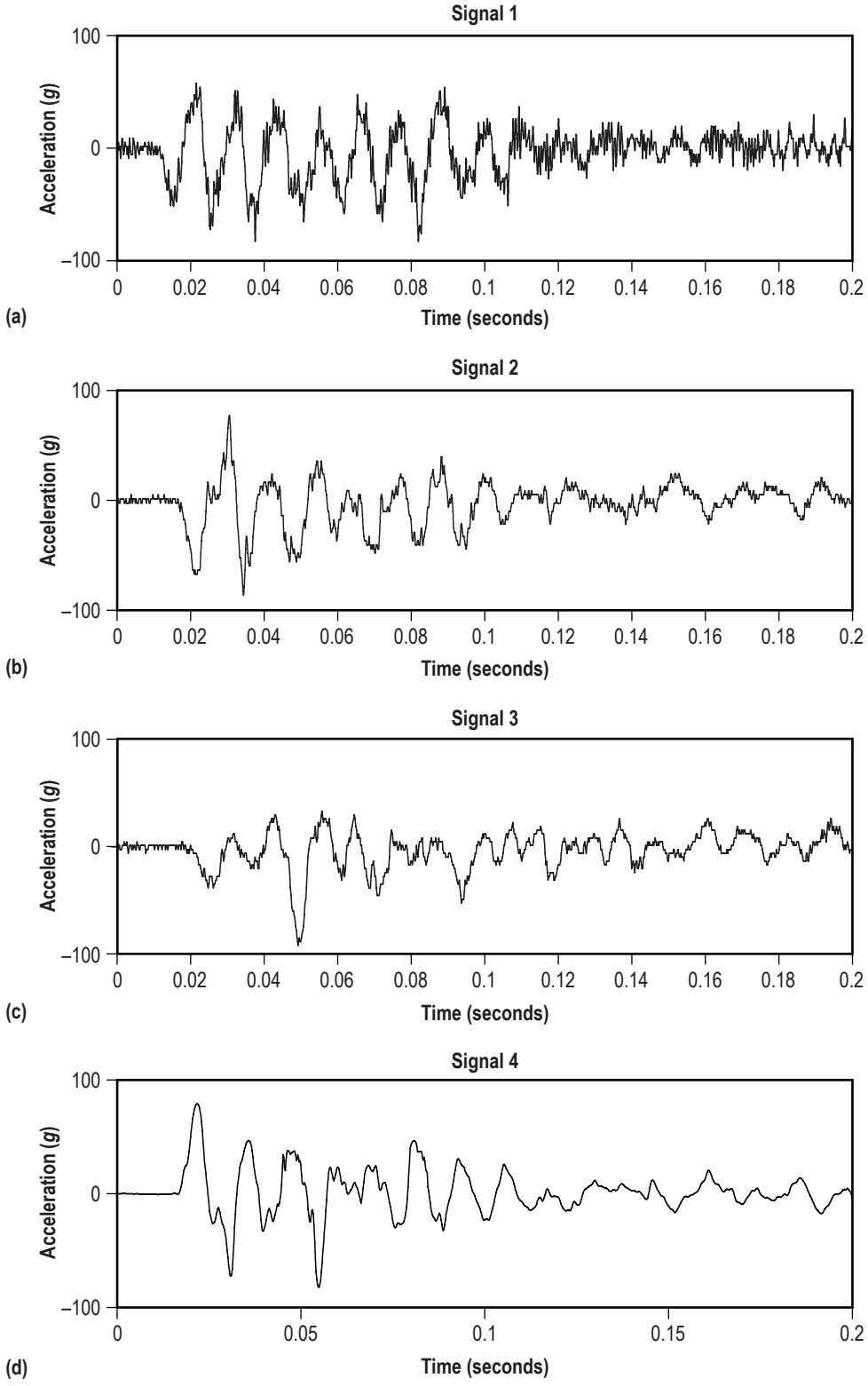

Figure 13. Measured acceleration time histories.

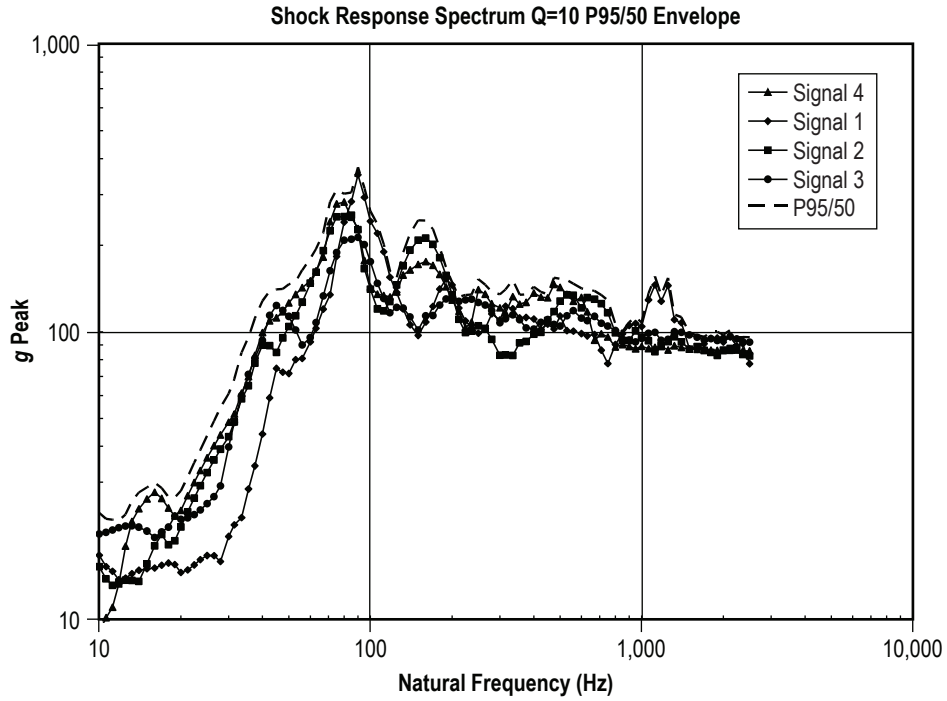

Figure 14. Shock response.

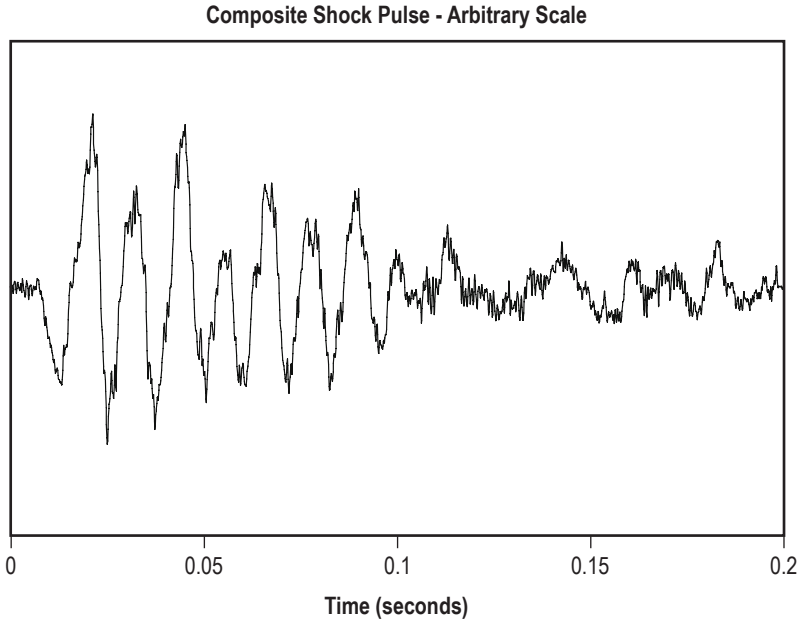

Figure 15. Composite shock pulse.

The approach is as follows:

(1) Add the measured time histories to form a single composite pulse, as seen in appendix E.
(2) Synthesize a wavelet time history to match the composite signal.
(3) Calculate the SRS of the synthesized wavelet series.

(4) Compare the wavelet SRS to the measured P95/50 SRS.
(5) Scale the wavelet components so that the two SRS curves agree within tolerance bands.
(6) Verify that the rescaled synthesized time history resembles each of the measured signals.

Note that steps (3) through (5) are repeated over hundreds of iterations. The resulting unscaled composite pulse for step (1) is shown in figure 15. The scaled synthesized wavelet acceleration pulse is given in figure 16. The corresponding velocity and displacement time histories are given in figures 17 and 18, respectively. The SRS comparison is given in figure 19.

Figure 15 shows the composite of the four measured signals from figure 13. The scale is arbitrary. The composite consists of 120 individual wavelets.

The scaled wavelet pulse in figure 16 qualitatively resembles the unscaled pulse in figure 15.

The velocity pulse is integrated from the acceleration pulse and is shown in figure 17. The net velocity is zero.

The net displacement (fig. 18) is zero. The peak displacement may be too high for certain shaker tables. It is based on an SRS specification that has a starting frequency at 10 Hz and the peak displacement could be reduced if the specification were to begin at 20 Hz, for example. Furthermore, optimization could be performed to reduce the peak displacement while still meeting the goals of 'acceleration time history resemblance' and SRS fulfillment.

The SRS of the scaled composite time history along with the tolerance bands (fig. 19) show that the spectra are very similar.

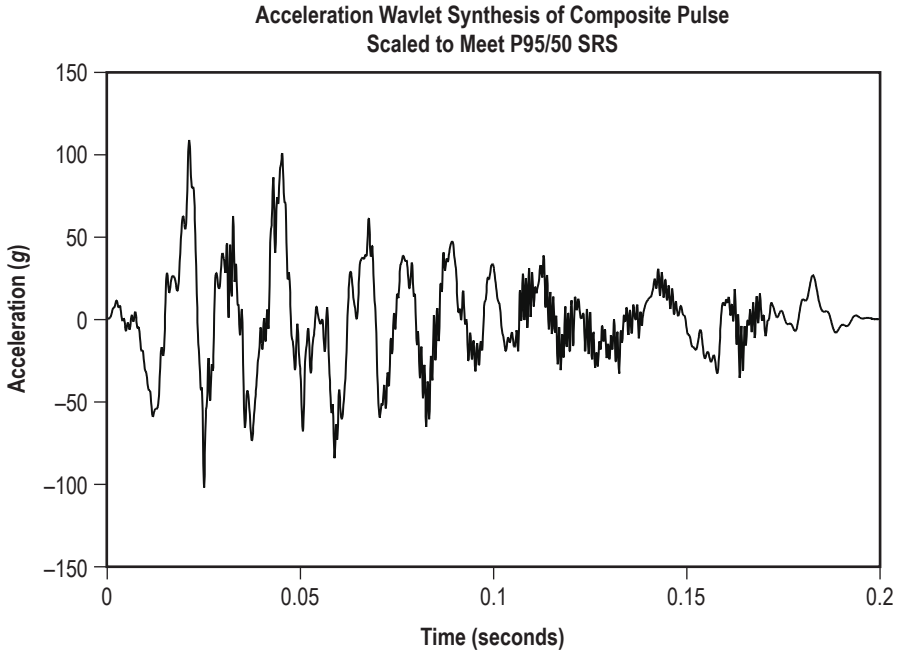

Figure 16. Acceleration wavelet synthesis.

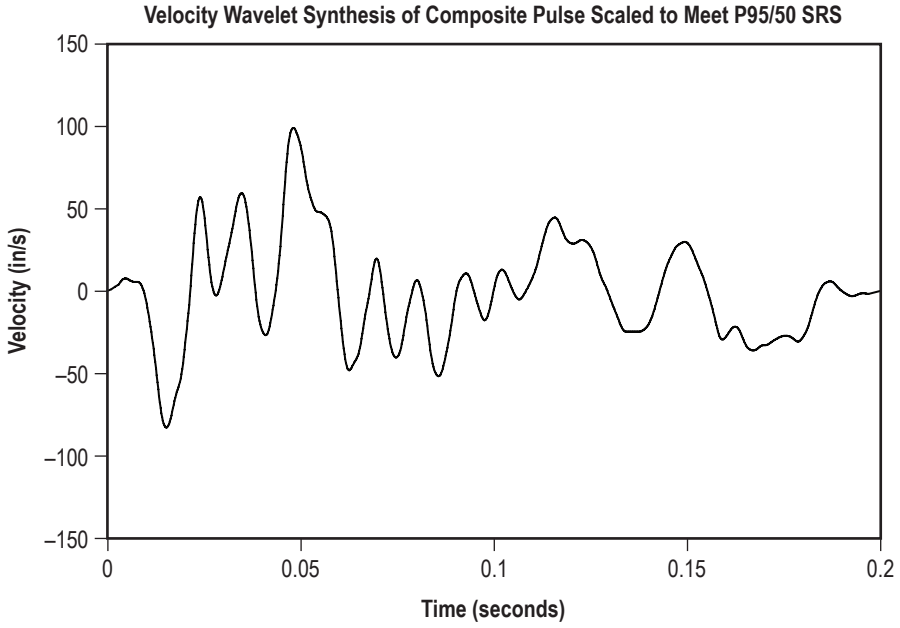

Figure 17. Velocity of wavelet synthesis.

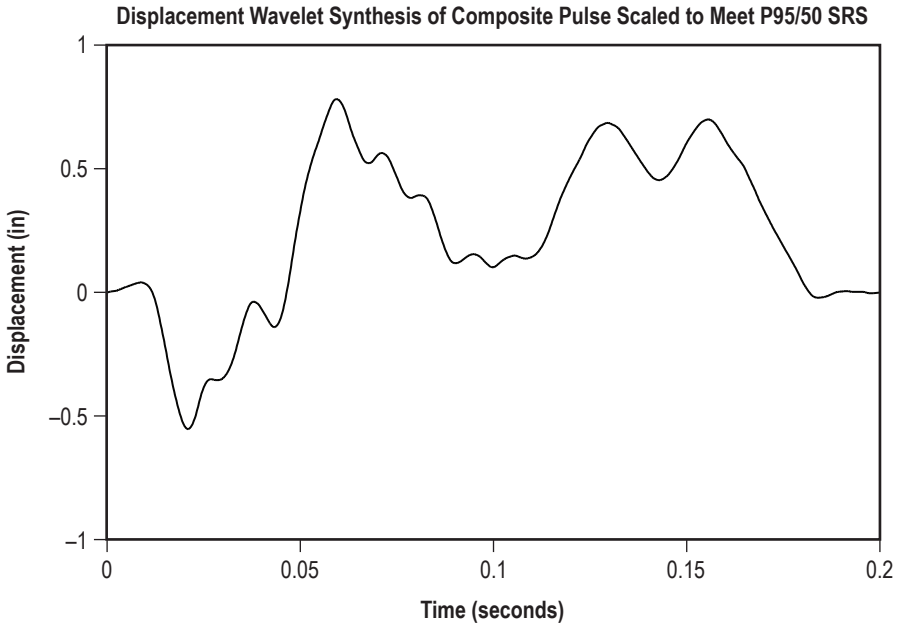

Figure 18. Displacement wavelet synthesis.

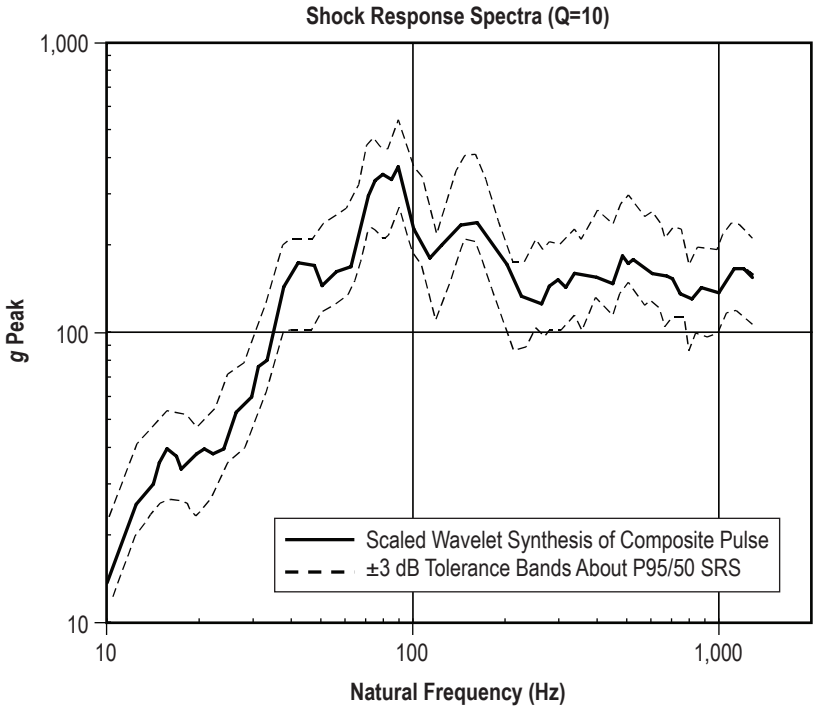

Figure 19. Shock response spectra.

4. CONCLUSION

This TM presented a method for synthesizing a time history to represent a measured time history using wavelets. In addition, the method was extended for the case of multiple measured time histories. A summary of the software programs used in the examples is given in appendix G. The wavelet time history may be applied to a test item via a shaker table with suitable frequency and amplitude limits. Test criteria would consist of a table of wavelets similar to that shown in appendix D, rather than an SRS. Any required margin could be imposed during the composite shock scaling process. Furthermore, the synthesized time history has a closed-form mathematical formula and the corresponding wavelet table may also be useful for identifying structural modal frequencies.

There will be a new series of impact qualification tests conducted in the near future as the Constellation Program gathers momentum. Current plans call for the Ares I first stage and Orion spacecraft to be reused. The Orion spacecraft is expected to impact on land, and SRS levels will be high in the low-to-mid frequencies, which would lend itself to this new technique to reduce the structural loads imposed by a traditional SRS approach.

The following concerns will be addressed in future research:

(1) The brute force method can be made more efficient using convergence algorithms, perhaps drawing from the field of genetics.

(2) Optimization could be performed to reduce the peak displacement while still meeting the goals of ‘acceleration time history resemblance’ and SRS fulfillment.

(3) The test fixture may have different mechanical impedance than the actual mounting surface in the vehicle.

APPENDIX A—RECONSTRUCTION OF WAVEFORMS FOR TRANSIENTS

Excerpt from Reference 1.

6.6 Reconstruction of Waveforms for Transients. The maximum expected environment (MEE) for transients is commonly computed in the frequency domain using the procedures detailed in Sections 6.1 through 6.4, where the MEE represents a conservative limit for a collection of measured or predicted spectra defining the transient environment in a structural zone of concern. Either Fourier spectra, energy spectra, or shock response spectra, as defined in Sections 2.2.8 through 2.2.10, might be used to compute the MEE. On the other hand, some of the test procedures discussed in Section 10, particularly those applicable to low frequency (below 100 Hz) transient simulations on electrodynamic shakers require a time history (waveform) for the specified test signal. When the MEE is defined in terms of a shock response spectrum (SRS), there is no direct analytical way to reconstruct a representative waveform because the SRS does not have a unique relationship to the waveform from which it is computed. For this case, test time history signals with an appropriate waveform are usually constructed using decaying sine waves [6.34 - 6.36] or wavelets [6.35, 6.36] ([6.36] includes Fortran programs). Also, energy spectra do not lend themselves to waveform reconstruction because they have no phase information. It follows that Fourier spectra should be used to define the MEE for transients when the reconstruction of a waveform is required for test simulation purposes.

APPENDIX B—WAVELET VELOCITY AND DISPLACEMENT

B.1 Wavelet Velocity

The equation for an individual acceleration wavelet over time t is

$$W_m(t) = \begin{cases} 0, \quad \text{for } t < t_{dm} \\ A_m \sin\left[\frac{2\pi f_m}{N_m}\left(t - t_{dm}\right)\right] \sin\left[2\pi f_m\left(t - t_{dm}\right)\right], \quad \text{for } t_{dm} \le t \le \left[t_{dm} + \frac{N_m}{2 f_m}\right] \\ 0, \quad \text{for } t > \left[t_{dm} + \frac{N_m}{2 f_m}\right] \end{cases} \tag{3}$$

where

$W_m(t)$ = acceleration of wavelet m at time t
A_m = wavelet acceleration amplitude
f_m = wavelet frequency
N_m = number of half-sines
t_{dm} = wavelet time delay

The velocity $V_m(t)$ at time t is as follows:

$$V_m(t) = \int_{t_{dm}}^{t} A_m \sin\left[\frac{2\pi f_m}{N_m}\left(t - t_{dm}\right)\right] \sin\left[2\pi f_m\left(t - t_{dm}\right)\right] dt \ , \quad \text{for } t_{dm} \le t \le \left[t_{dm} + \frac{N_m}{2 f_m}\right] \tag{4}$$

Let

$u = t - t_{dm}$

$du = dt$

$$\alpha = \frac{2\pi f_m}{N_m}$$

$$\beta = 2\pi f_m$$

$$V_m(t) = A_m \int_{u_1}^{u_2} \sin\left[\alpha u\right] \sin\left[\beta u\right] du \tag{5}$$

$$V_m(t) = -\frac{1}{2} A_m \int_{u_1}^{u_2} \cos\left[\left(\alpha + \beta\right)u\right] du + \frac{1}{2} A_m \int_{u_1}^{u_2} \cos\left[\left(\alpha - \beta\right)u\right] du \tag{6}$$

$$V_m(t) = -\frac{A_m}{2\left(\alpha + \beta\right)} \sin\left[\left(\alpha + \beta\right)u\right]\Big|_{u_1}^{u_2} + \frac{A_m}{2\left(\alpha - \beta\right)} \sin\left[\left(\alpha - \beta\right)u\right]\Big|_{u_1}^{u_2} \tag{7}$$

$$V_m(t) = -\frac{A_m}{2\left(\alpha + \beta\right)} \sin\left[\left(\alpha + \beta\right)\left(\tau - t_{dm}\right)\right]\Big|_{t_{dm}}^{t} + \frac{A_m}{2\left(\alpha - \beta\right)} \sin\left[\left(\alpha - \beta\right)\left(\tau - t_{dm}\right)\right]\Big|_{t_{dm}}^{t} \tag{8}$$

The wavelet velocity equation is as follows:

$$V_m(t) = -\frac{A_m}{2\left(\alpha + \beta\right)} \sin\left[\left(\alpha + \beta\right)\left(t - t_{dm}\right)\right] + \frac{A_m}{2\left(\alpha - \beta\right)} \sin\left[\left(\alpha - \beta\right)\left(t - t_{dm}\right)\right] , \tag{9}$$

$$\text{for } t_{dm} \le t \le \left[t_{dm} + \frac{N_m}{2 f_m}\right]$$

The wavelet ends at

$$t = \left[t_{dm} + \frac{N_m}{2 f_m}\right] = \left[t_{dm} + \frac{\pi}{\alpha}\right] \tag{10}$$

The velocity at the end time is

$$V_m\left(t_{dm} + \frac{\pi}{\alpha}\right) = -\frac{A_m}{2\left(\alpha + \beta\right)} \sin\left[\left(\alpha + \beta\right)\left(\left(t_{dm} + \frac{\pi}{\alpha}\right) - t_{dm}\right)\right] \tag{11}$$

$$+ \frac{A_m}{2\left(\alpha - \beta\right)} \sin\left[\left(\alpha - \beta\right)\left(\left(t_{dm} + \frac{\pi}{\alpha}\right) - t_{dm}\right)\right]$$

$$V_m\left(t_{dm}+\frac{\pi}{\alpha}\right)=-\frac{A_m}{2(\alpha+\beta)}\sin\left[\left(1+\frac{\beta}{\alpha}\right)\pi\right]+\frac{A_m}{2(\alpha-\beta)}\sin\left[\left(1-\frac{\beta}{\alpha}\right)\pi\right] \tag{12}$$

Note that $\frac{\beta}{\alpha} = N_m$, an odd integer ≥3. (13)

Thus,

$$\sin\left[\left(1+\frac{\beta}{\alpha}\right)\pi\right]=0 \tag{14}$$

$$\sin\left[\left(1-\frac{\beta}{\alpha}\right)\pi\right]=0 \tag{15}$$

The net velocity is as follows:

$$V_m\left(t_{dm}+\frac{\pi}{\alpha}\right)=0 \tag{16}$$

B.2 Wavelet Displacement

The wavelet displacement $D_m(t)$ for wavelet m is obtained by integrating the velocity. (17)

$$D_m(t)=-\frac{A_m}{2(\alpha+\beta)}\int_{t_{dm}}^{t}\sin\left[(\alpha+\beta)(t-t_{dm})\right]dt+\frac{A_m}{2(\alpha-\beta)}\int_{t_{dm}}^{t}\sin\left[(\alpha-\beta)(t-t_{dm})\right]dt\ , \tag{18}$$

$$\text{for}\ \ t_{dm}\le t\le\left[t_{dm}+\frac{N_m}{2f_m}\right]$$

Again,

$$\alpha=\frac{2\pi f_m}{N_m} \tag{19}$$

$$\beta=2\pi f_m \tag{20}$$

$$D_m(t)=+\frac{A_m}{2(\alpha+\beta)^2}\cos\left[(\alpha+\beta)(t-t_{dm})\right]\Big|_{t_{dm}}^{t}-\frac{A_m}{2(\alpha-\beta)^2}\cos\left[(\alpha-\beta)(t-t_{dm})\right]\Big|_{t_{dm}}^{t} \tag{21}$$

The displacement equation is

$$D_m(t) = + \frac{A_m}{2\left(\alpha+\beta\right)^2}\left\{\cos\left[\left(\alpha+\beta\right)\left(t-t_{dm}\right)\right]-1\right\} - \frac{A_m}{2\left(\alpha-\beta\right)^2}\left\{\cos\left[\left(\alpha-\beta\right)\left(t-t_{dm}\right)\right]+1\right\} \quad , \quad (22)$$

$$\text{for } t_{dm} \le t \le \left[t_{dm} + \frac{N_m}{2f_m}\right]$$

The wavelet ends at $t = \left[t_{dm} + \frac{N_m}{2f_m}\right] = \left[t_{dm} + \frac{\pi}{\alpha}\right]$ (23)

The final displacement is as follows:

$$D_m(t_{dm} + \frac{\pi}{\alpha}) = + \frac{A_m}{2\left(\alpha+\beta\right)^2}\left\{\cos\left[\left(1+\frac{\beta}{\alpha}\right)\pi\right]-1\right\} - \frac{A_m}{2\left(\alpha-\beta\right)^2}\left\{\cos\left[\left(1-\frac{\beta}{\alpha}\right)\pi\right]+1\right\} \quad (24)$$

Note that $\frac{\beta}{\alpha} = N_m$, an odd integer ≥3. (25)

Thus,

$$\cos\left[\left(1+\frac{\beta}{\alpha}\right)\pi\right]-1=0 \quad (26)$$

$$\cos\left[\left(1-\frac{\beta}{\alpha}\right)\pi\right]-1=0 \quad (27)$$

The net displacement is as follows:

$$D_m\left(t_{dm}+\frac{\pi}{\alpha}\right)=0 \quad (28)$$

APPENDIX C—WAVELET TABLE FOR FIRST EXAMPLE

The wavelet synthesis in Figure 8b is composed of the individual wavelet components in Table 2.

Table 2. Wavelet synthesis components.

Acceleration (*g*)	Frequency (Hz)	NHS	Delay (s)	Acceleration (*g*)	Frequency (Hz)	NHS	Delay (s)
31.42	74.59	9	0.0119	4.64	593.45	27	0.0418
24.41	80.76	17	0.0232	–8.86	273.93	5	0.0826
–23.19	44.74	3	0.0128	–4.29	102.91	3	0.1354
20.38	149.91	7	0.0159	4.87	532.84	23	0.0563
–14.22	41.27	7	0.1072	–4.06	93.69	7	0.0560
–19.50	63.18	5	0.0285	–5.22	314.89	15	0.0263
–10.55	124.46	19	0.0242	6.51	146.43	3	0.0478
–5.60	83.75	19	0.0306	7.61	765.69	7	0.0688
9.76	55.67	3	0.0086	–3.78	135.14	7	0.0046
6.28	73.98	9	0.1353	–3.38	113.53	9	0.1584
–4.04	38.95	13	0.0125	–2.75	91.92	9	0.1496
6.99	153.87	11	0.0163	3.37	469.06	21	0.0430
4.24	55.43	13	0.0789	5.85	698.73	13	0.0862
–9.02	98.88	5	0.0902	–5.34	865.48	13	0.0306
10.44	168.46	7	0.0591	5.38	383.49	11	0.1214
–3.79	16.36	5	0.0048	–1.89	19.78	5	0.0010
12.22	325.26	9	0.0620	–6.43	1,034.55	9	0.0936
–12.66	426.15	3	0.0332	–6.26	312.02	3	0.1454
–9.35	360.30	19	0.0777	–2.20	133.06	21	0.0495
–10.63	609.62	13	0.0257	–4.42	290.23	7	0.1564
–3.96	97.17	9	0.1520	–4.39	1343.20	21	0.0406
–6.34	157.05	17	0.1399	5.74	992.92	11	0.0784
5.93	230.17	17	0.0250	2.83	282.84	11	0.0664
–4.00	57.68	5	0.0160	1.48	49.99	17	0.0166
–4.88	153.39	15	0.0776	2.29	263.19	13	0.0081
–1.58	26.43	9	0.0166	2.08	63.73	5	0.1576
7.24	434.76	13	0.0253	2.33	35.77	3	0.1567
8.64	627.99	9	0.0209	–5.70	379.76	5	0.0934
–7.81	335.76	7	0.1347	2.99	45.05	3	0.0003
8.85	345.89	7	0.1126	4.54	1,334.48	27	0.0827

The first wavelet is shown in figure 20.

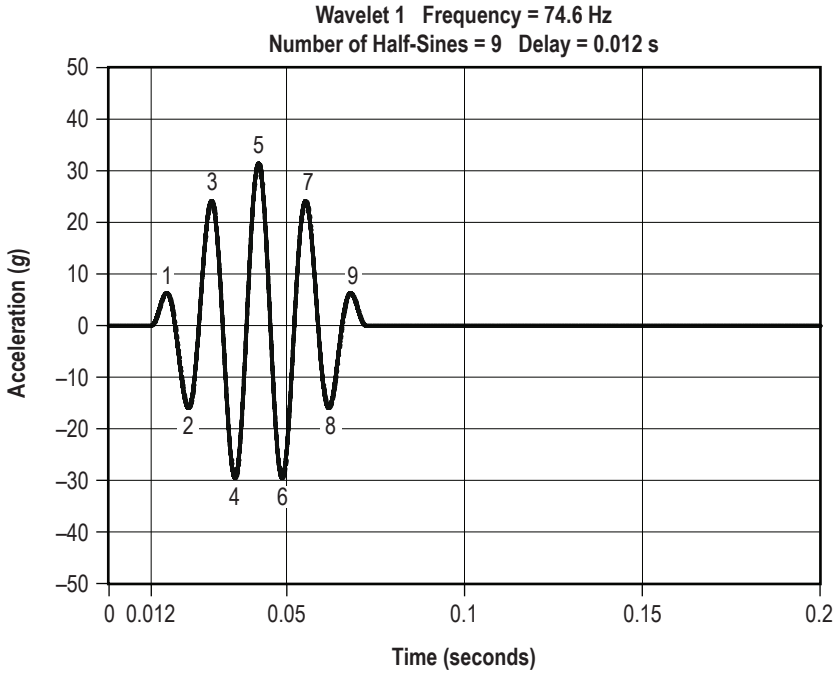

Figure 20. Wavelet 1.

An equivalent acceleration formula for equation (1) is as follows:

$$W_m(t) = -\frac{A_m}{2}\cos\left[2\pi f_m\left(\frac{1}{N_m}+1\right)\left(t-t_{dm}\right)\right]+\frac{A_m}{2}\cos\left[2\pi f_m\left(\frac{1}{N_m}-1\right)\left(t-t_{dm}\right)\right] \quad , \qquad (29)$$

$$\text{for } t_{dm} \le t \le \left[t_{dm}+\frac{N_m}{2f_m}\right]$$

Obviously, a given wavelet has a beat frequency effect with two spectral lines over the defined interval. The corresponding spectral magnitude function of the waveform in equation (29) is shown in figure (21).

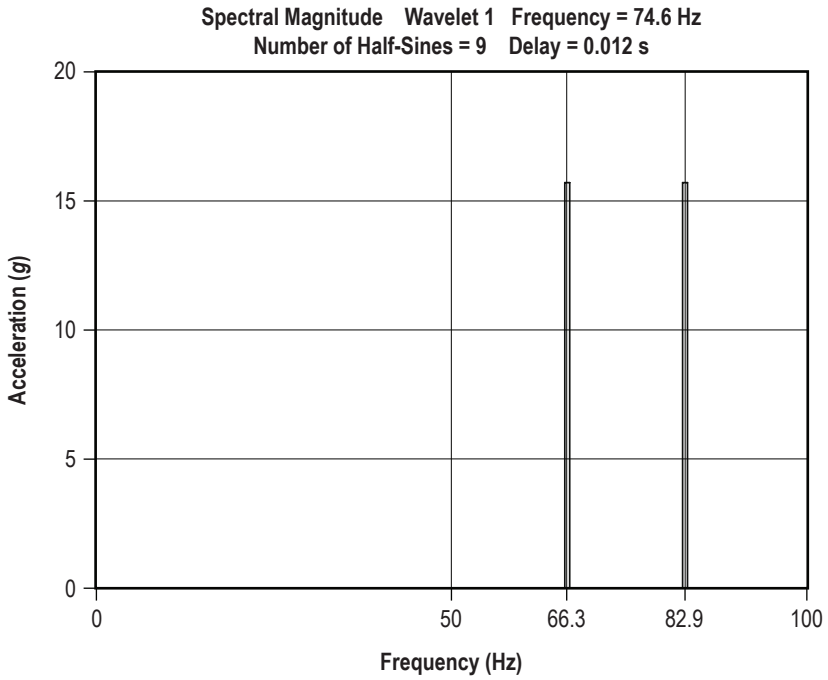

Figure 21. Wavelet 1 Spectrum.

The spectral magnitude function is somewhat analogous to a Fourier transform magnitude. An actual Fourier transform of the data would be of limited value since the energy would be smeared over several frequencies due to 'leakage' and other error sources. Note that the frequency increment of a Fourier transform is equal to the reciprocal of the signal duration. A Fourier transform is thus more suitable for data sets with longer durations.

APPENDIX D—MAXIMUM PREDICTED LEVEL

The P95/50 rule yields the maximum predicted level, which is equal to or greater than the value at the 95th percentile at least 50% of the time. The '95' in the P95/50 rule is taken as the 95% probability in the normal distribution. The '50' is the 50% confidence value in the chi-square distribution. The tolerance value is applied to the sample standard deviation to yield an estimate of the upper limit at each frequency as follows:

$$\text{Limit} = \bar{x} + ks \tag{30}$$

where $\bar{x}$ is the mean and s is the sample standard deviation. K-factors for a 95% and 97.5% probability level (PL) are shown in table 3.

Table 3. Tolerance factors for various probability levels.

	95% PL	97.5% PL
n	K-Factor	K-Factor
2	2.193	2.613
3	1.880	2.240
4	1.794	2.138
5	1.755	2.091
6	1.731	2.063
7	1.716	2.045
8	1.706	2.033
9	1.698	2.023
10	1.692	2.016
11	1.687	2.010
12	1.683	2.006
13	1.680	2.002
14	1.677	1.998
15	1.675	1.996
20	1.667	1.986
25	1.662	1.981
30	1.659	1.977
40	1.655	1.973
50	1.653	1.970
60	1.652	1.968
70	1.651	1.967
100	1.649	1.965
∞	1.645	1.960

APPENDIX E—SUMMING ACCELEROMETER SIGNALS

Creating a Composite Pulse

The composite pulse is the sum of several individual signals. The raw signals, however, cannot be simply added together. There are several concerns that must be addressed so that a reasonable sum is achieved.

Accelerometer Mounting

Consider a pair of accelerometers mounting in the same axis. The accelerometers may or may not be mounted with the same polarity. In other words, one accelerometer may be mounted in the positive axis and the other in the negative axis. If so, the signal from one accelerometer would be inverted with respect to the other signal, assuming that the waveform is simultaneous and in-phase at each location. Note that in some cases, the accelerometer mounting diagram may not be readily available to the engineer who is reducing the measured data.

Field Types

Another concern arises from the distance of the accelerometers with respect to the source location, as well as the distance between the accelerometers themselves. Some shock events, such as pyrotechnic stage separation, may have a well-defined source location. Other events, such as water impact, may have a complex, distributed source. Regardless, the source shock has the potential of generating both traveling and standing waves. The standing waves represent modes. The ‘near-field’ response to a discrete shock source is dominated by waves. The ‘far-field’ response is largely due to structural modes. The ‘mid-field’ response is a combination of each type.

Response to Traveling Waves

Consider a wave-like response that is measured at two accelerometer locations. There may be a measurable time delay between the two responses if the accelerometers are mounted sufficiently apart from one another. Obviously, the speed of sound in the material enters into this calculation. Furthermore, the wave speed varies depending on the wave type. The wave speed may even vary with frequency, as is the case with traveling bending waves. Similarly, dispersion may occur.

Modal Response

There are three main scenarios for two accelerometers measuring a given vibration mode.

(1) The accelerometers may be in-phase.
(2) The accelerometers may be 180 degrees out-of-phase.
(3) Either accelerometer may be on a nodal line.

Either destructive or constructive interference may result from adding the signals. Furthermore, the magnitude of the response at each location may vary regardless of phase.

Filtering

The telemetry data may have been filtered in some manner that introduces a phase delay.

Synchronization

Accelerometer data from more than one flight may be available. The data may or may not be synchronized to a common starting time. The 'true starting time' may be a matter of engineering judgment.

Summation

As a result of these concerns, there is no exact method for summing accelerometer signals for the purpose of deriving a composite pulse. Again, brute force random number generation may be used. One method is to multiply each signal by +1 or –1, then shift each signal by some 'small' time delay. Each of these steps is performed in a random manner over hundreds of trials. The final composite pulse is the one that yields the greatest root mean square (RMS) value.

A possible concern is that this approach may emphasize certain modal frequency while attenuating others. Again, the wavelet components are rescaled to meet the P95/50 SRS, as explained in the main text. Thus, all frequency components should be represented to the proper amplitude in the final wavelet series.

APPENDIX F—SOFTWARE PROGRAMS

The program files are included in the initial submission of this TM to the customer and are listed in table 4 below. Other interested parties may contact the Tom Irvine at Vibration Data, LLC. (*http://vibrationdata.com/*) for copies of the code. The programs are DOS or 'console mode.' Also, the programs are nearly straight C, rather than C++. The programs were written using Microsoft® Visual C++ 6.0; however, they do not use any Graphical User Interfaces or Visual features. Some minor changes may be required for other compilers.

Table 4. Applicable software programs.

Program	Description
wavelet_reconstruct.cpp	Synthesizes a wavelet series to represent a measured time history
composite_shock.cpp	Adds multiple waveforms using inversion and time delays to maximize the RMS
srs_9550.cpp	Calculates the P95/50 level for two or more shock response spectra
wavelet_scale_SRS.cpp	Scales the individual wavelets of a series so that the resulting time history satisfies an SRS specification
th_from_wavelet_table.cpp	Generates a time history from a wavelet table
qsrs.cpp	Calculates an SRS for an acceleration time history

REFERENCES

1. Smith, S.; and Hollowell, B: "A Proposed Method to Standardize Shock Response Spectrum (SRS) Analysis." *Journal of the Institute of Environmental Sciences*, May/June 1996.

2. Scavuzzo, R.J.; and Pusey, H.C.: *Naval Shock Analysis and Design*, 2nd ed., 2002.

3. "Force Limited Vibration Testing," NASA-HDBK-7004B, Jet Propulsion Laboratory, CA, 2003.

4. Himelblau, H.; Kern, D.L.; and Piersol, A.G.; et al.: "Dynamic Environmental Criteria," NASA-HDBK-7005, Jet Propulsion Laboratory, CA, 2001.

REPORT DOCUMENTATION PAGE

Form Approved
OMB No. 0704-0188

1. AGENCY USE ONLY *(Leave Blank)*	2. REPORT DATE	3. REPORT TYPE AND DATES COVERED
	April 2008	Technical Memorandum

4. TITLE AND SUBTITLE

An Alternative Method of Specifying Shock Test Criteria

5. FUNDING NUMBERS

NAS8–02045

6. AUTHORS

R.C. Ferebee, J. Clayton,* D. Alldredge,* and T. Irvine**

7. PERFORMING ORGANIZATION NAME(S) AND ADDRESS(ES)

George C. Marshall Space Flight Center
Marshall Space Flight Center, AL 35812

8. PERFORMING ORGANIZATION REPORT NUMBER

M–1226

9. SPONSORING/MONITORING AGENCY NAME(S) AND ADDRESS(ES)

National Aeronautics and Space Administration
Washington, DC 20546–0001

10. SPONSORING/MONITORING AGENCY REPORT NUMBER

NASA/TM—2008–215253

11. SUPPLEMENTARY NOTES

Prepared by the Chief Engineers Office, Engineering Directorate
* bd Systems, Inc./Subsidiary of SAIC, Huntsville, AL, ** Vibration Data, LLC., Chandler, AZ

12a. DISTRIBUTION/AVAILABILITY STATEMENT

Unclassified-Unlimited
Subject Category: 39
Availability: NASA CASI 301–621–0390

12b. DISTRIBUTION CODE

13. ABSTRACT *(Maximum 200 words)*

Shock testing of aerospace vehicle hardware has presented many challenges over the years due to the high magnitude and short duration of the specifications. Recently, component structural failures have occurred during testing that have not manifested themselves on over 200 Space Shuttle solid rocket booster (SRB) flights (two boosters per flight). It is suspected that the method of specifying shock test criteria may be leaving important information out of the test process. The traditional test criteria specification, the shock response spectrum, can be duplicated by any number of waveforms that may not resemble the actual flight test recorded time history. One method of overcoming this limitation is described herein, which may prove useful for qualifying hardware for the upcoming Constellation Program.

14. SUBJECT TERMS

shock testing, shock test criteria, waveform reconstruction

15. NUMBER OF PAGES

44

16. PRICE CODE

17. SECURITY CLASSIFICATION OF REPORT	18. SECURITY CLASSIFICATION OF THIS PAGE	19. SECURITY CLASSIFICATION OF ABSTRACT	20. LIMITATION OF ABSTRACT
Unclassified	Unclassified	Unclassified	Unlimited

National Aeronautics and
Space Administration
IS20
George C. Marshall Space Flight Center
Marshall Space Flight Center, Alabama
35812